REPORT DOCUMENTATION PAGE

Form Approved
OMB No. 0704-0188

1. REPORT DATE *(DD-MM-YYYY)*	2. REPORT TYPE	3. DATES COVERED *(From - To)*
10-08-2005	Conference Proceeding (not refereed)	

4. TITLE AND SUBTITLE
Wavenumber Spectrum of Intermediate-scale Ocean Surface Waves

5a. CONTRACT NUMBER

5b. GRANT NUMBER

5c. PROGRAM ELEMENT NUMBER
0602435N

6. AUTHOR(S)
Hwang, Paul A.

5d. PROJECT NUMBER

5e. TASK NUMBER

5f. WORK UNIT NUMBER
73-6628-85-5

7. PERFORMING ORGANIZATION NAME(S) AND ADDRESS(ES)
Naval Research Laboratory
Oceanography Division
Stennis Space Center, MS 39529-5004

8. PERFORMING ORGANIZATION REPORT NUMBER
NRL/PP/7330--05-5202

9. SPONSORING/MONITORING AGENCY NAME(S) AND ADDRESS(ES)
Office of Naval Research
800 N. Quincy St.
Arlington, VA 22217-5660

10. SPONSOR/MONITOR'S ACRONYM(S)
ONR

11. SPONSOR/MONITOR'S REPORT NUMBER(S)

12. DISTRIBUTION/AVAILABILITY STATEMENT
Approved for public release, distribution is unlimited.

13. SUPPLEMENTARY NOTES

14. ABSTRACT
This paper presents an analysis of the wavenumber spectra of intermediate-scale waves (wavelengths between 0.02 and 6 m) under various sea-state conditions. The main result of the analysis is that the dependence of the dimensionless wave spectrum on the dimensionless wind-friction velocity follows a power-law function. The coefficient and exponent of the power-law function vary systematically with the wavenumber. The wavenumber dependence of the coefficient and exponent serves as an empirical parameterization for computing the wavenumber spectra of intermediate-scale waves at different wind speeds. Calculation of the mean-square slope from the resulting wavenumber spectrum confirms that intermediate-scale waves are the dominate contributor of the ocean surface roughness. A simple formula is presented for calculating the band-pass filtered mean-square slope of the ocean surface for remote sensing applications.

15. SUBJECT TERMS
wavenumber spectra; dimensionless wave spectrum; dimensionless wind-friction velocity; power-law function

16. SECURITY CLASSIFICATION OF:			17. LIMITATION OF ABSTRACT	18. NUMBER OF PAGES	19a. NAME OF RESPONSIBLE PERSON
a. REPORT	b. ABSTRACT	c. THIS PAGE			Paul A. Hwang
Unclassified	Unclassified	Unclassified	UL	4	19b. TELEPHONE NUMBER *(Include area code)* 228-688-4708

Wavenumber spectrum of intermediate-scale ocean surface waves

Paul A. Hwang
Oceanography Division, Naval Research Laboratory, Stennis Space Center, MS, 39529 USA

*Abstract - **This paper presents an analysis of the wavenumber spectra of intermediate-scale waves (wavelengths between 0.02 and 6 m) under various sea-state conditions. The main result of the analysis is that the dependence of the dimensionless wave spectrum on the dimensionless wind friction velocity follows a power-law function. The coefficient and exponent of the power-law function vary systematically with the wavenumber. The wavenumber dependence of the coefficient and exponent serves as an empirical parameterization for computing the wavenumber spectra of intermediate-scale waves at different wind speeds. Calculation of the mean-square slope from the resulting wavenumber spectrum confirms that intermediate-scale waves are the dominant contributor of the ocean surface roughness. A simple formula is presented for calculating the band-pass filtered mean-square slope of the ocean surface for remote sensing applications.***

I. INTRODUCTION

Surface waves a few centimeters to a few meters long (referred to as the intermediate-scale waves hereafter) are generally believed to be the dominant contributor of the ocean surface roughness. So far, reliable measurements of intermediate-scale waves in the ocean environment are essentially nonexistent. As a result, verification of that assumption based on field data has not yet presented. Due to the large Doppler frequency shift when traditional point-measurement systems are employed, the measurement accuracy of intermediate-scale waves in the ocean is difficult to assess. Most ocean wave data focus on the energy-containing frequency band in the neighborhood of the displacement spectral peak. A small fraction of the wave data focuses on the length scale of gravity-capillary waves, using mainly optical scanning sensors to conduct spatial measurements to avoid the tricky problems associated with the Doppler frequency shift [e.g., 1-2]. Extending optical scanning techniques to wave components several meters long for field applications is prohibitively expensive and impractical. Ref. [1] suggested that the problem of Doppler frequency shift can be alleviated by using a free-drifting measurement technique. The effectiveness of removing Doppler frequency shift by free-drifting operations was demonstrated by comparing the wavenumber-frequency spectra measured by linear arrays of wire gauges deployed in free-drifting and fixed-station configurations [3] and reliable conversion of the wave spectrum from frequency to wavenumber domain can be expanded into intermediate-scale wave components.

Ref. [3] presented an analysis of field measurements of intermediate-scale waves. Following the suggestion by Ref. [4], the data were processed to investigate the empirical functional dependence of the dimensionless spectrum, $B(k)$, on the dimensionless wind friction velocity, u_*/c, where k is the wavenumber and c is the wave phase speed. The result shows that $B(k)$ can be expressed as a power-law function of u_*/c. The coefficient and exponent of the power-law function are wavenumber dependent. In this paper, using the above result serving as an empirical parameterization function, the wavenumber spectra of intermediate-scale waves at different wind speeds are quantified (Section II). The properties of the mean-square slopes integrated over different wavenumber ranges are investigated in Section III. A summary is given in Section IV.

II. EMPIRICAL PARAMETERIZATION

In a discussion of the source function balance of short ocean surface waves that are important to remote sensing applications, Ref. [4] emphasized that the knowledge on the variation of the wavenumber spectrum with wind speed can provide valuable information on the properties of the dissipation function. Ref. [3] reported an analysis of the wave spectra collected in the ocean using a free-drifting technique. The spectra are divided into two different groups: wind seas and mixed seas. The range of wind speeds is 3.6 to 14.2 m/s for the former group (291 cases), and 2.6 to 10.2 m/s for the latter group (106 cases). For each wave component, the scatter plot of $B(k)$ as a function of u_*/c shows a general power-law dependence,

$$B\left(\frac{u_*}{c};k\right) = A_0(k)\left(\frac{u_*}{c}\right)^{a_0(k)}. \qquad (1)$$

The coefficient and exponent of the power-law function for each wave component can be calculated from least-square fitting of the ocean data. The variations of A_0 and a_0 with k are depicted in Figs. 1a and 1b, respectively. Ref. [3] presented fifth-order polynomial

fitting functions for A_0 and a_0 but the polynomial functions obviously missed many fine features of the variations (see their Fig. 3). Here the computation is carried out by using a lookup table interpolating through the measured data, the interpolated curves capture most of the subtle details of the variations in A_0 and a_0 (compare the continuous curves and discrete data in Figs. 1a-b). For the range $1<k<2$ rad/m, the scatter of the mixed-sea data is large and the wind-sea data in this range are used for both wind seas and mixed seas.

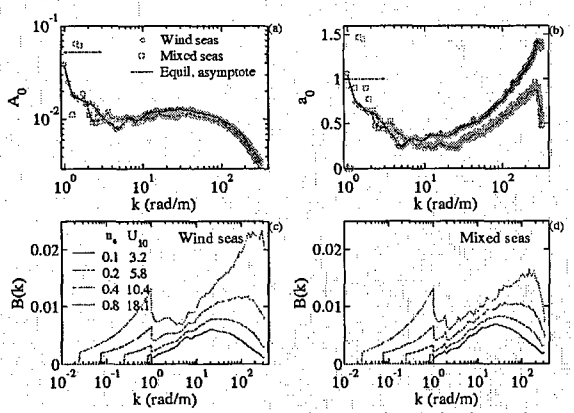

Fig. 1. (a) A_0, and (b) a_0 of the power-law function derived from least-square fitting of field data. $B(k)$ computed from the parameterization function (1) using table lookup for A_0 and a_0: (c) Wind seas, and (b) mixed seas.

Fig. 1c-d displays the computed wavenumber spectra over a range of wind speeds using the parameterization function (1) for the wavenumber range $1 \le k \le 316$ rad/m. The semilogarithmic plots in the top panels represent the area-conservation representation of the mean-square slope of the ocean surface, that is, the area under the curve over a range of wavenumbers represents the mean-square slope of the corresponding spectral wave components, because for the omni-directional spectrum $B(k)=kS_1(k)$, where S_1 is the omni-directional wave slope spectrum (Appendix of Ref. [5]). The results for the wind seas are plotted in Fig. 1c and those for the mixed seas in Fig. 1d. The background ocean waves modify the spectrum of intermediate-scale waves in a somewhat complex way. For waves shorter than about 1 m, the background waves enhance the spectral densities of intermediate-scale waves at lower wind speeds but reduce their spectral densities at higher wind speeds. For longer intermediate-scale waves, the effect of background waves is opposite to that for the shorter waves. The magnitude of the spectral fluctuations deviating from the wind-sea condition is usually within about 20 percent for most intermediate-scale wave components in the available data. The critical wind speed separating these two opposite trends is somewhat higher than 6 m/s. Interestingly, the wind speed 7 m/s is frequently associated with the inception of more-intensive breaking events in the ocean and the transition of the surface roughness condition from smooth to hydrodynamically rough. The results shown in Fig. 2c may reflect the influences of breaking wave and surface roughness conditions on the intermediate-scale waves. The detailed effects of wave breaking and roughness conditions on the properties of short- and intermediate-scale waves in the ocean are not well understood. Theoretical investigations on related subjects have indicated that the mechanisms of wave-turbulence interaction and wave breaking exert strong impact on the air-sea momentum transfer and wind-wave generation [e.g., 6-7]. From the empirical data gathered here, it is found that the response of wave components between 1 and 2 m long to the background waves is opposite to that of shorter waves. The data quality of wave components longer than 3 m ($1<k<2$ rad/m) in the present dataset is not very good for the mixed-sea conditions, judging from the large data scatter of A_0 and a_0 in this wavenumber range shown in Figs. 1a-b, and it is difficult to determine the influence of background waves on the longer components of intermediate-scale waves.

For the wavenumber range $k_p<k<1$, where k_p is the wavenumber at the peak of the surface displacement spectrum, the equilibrium spectral function is assumed,

$$S_e(k) = bu_* g^{-0.5} k^{-2.5} = b\frac{u_*}{c} k^{-3}, \qquad (2)$$

where the spectral constant $b \approx 5.2\times10^{-2}$ is used, and g is the gravitational acceleration. The corresponding dimensionless spectrum is

$$B_e(k) = b\left(\frac{u_*}{c}\right). \qquad (3)$$

The results shown in Fig. 1c-d illustrate that intermediate-scale waves are the dominant contributor of the ocean surface mean-square slope. The peak of the distribution of mean-square slopes represented by $B(k)$ is near 20 rad/m at 3 m/s, and moves toward higher wavenumber as wind speed increases, reaching to about 200 rad/m at 18 m/s. The dropoff of the spectral densities at the higher wavenumber end (waves shorter than about 2 cm) is quite steep. There is an apparent kink at $k=1$ rad/m in merging $B(k)$ and $B_e(k)$, possibly due to the relatively simple equilibrium spectral model used here. This is not considered to be a significant drawback for the discussion of ocean surface roughness because the contribution of long gravity waves to the overall mean-square slope of the ocean surface is relatively small. The kink can be smoothed by interpolation using the spectral data in the neighborhood of $k=1$ rad/m. A simple linear interpolation is applied to $B(k)$ in the range $6k_p<k<1.2$ rad/m using values of $B(6k_p)$ and $B(1.2)$. No smoothing is applied if $6k_p \ge 1$ rad/m. The smoothing of the spectral

kink only introduced a minor change in the mean-square slope computation and does not alter the main conclusions discussed in this paper.

III. MEAN-SQUARE SLOPE

Using the wavenumber spectrum presented in the last section, the mean-square slope, s, of the ocean surface can be calculated. Because waves longer that the wavelength at the spectral peak make only negligible contribution to the total mean-square slope, the lower-bound wavenumber for integration is set at k_p. The highest wavenumber of the spectrum considered here is 316 rad/m, thus the mean-square slope computed in the following covers almost the full range of the gravity wave spectrum.

The results calculated for the upper-bound cutoff wavenumbers of 316, 63 and 21 rad/m (cutoff wavelengths 0.02, 0.1 and 0.3 m) for wind seas and mixed seas are shown in Fig. 2. For comparison, field data of the mean-square slopes obtained from the analyses of sun glitter [8] and airborne K_u-band radar backscattering cross sections [9] are superimposed in the figure. The sun glitter data are further divided into two groups, clean surface and artificial or manmade slicks. The slicks suppress short waves, and the cutoff wavenumber was estimated to be about 21 rad/m, that is, waves shorter than 0.3 m were suppressed [8]. The agreement between field data and computations appears to be reasonable considering the large scatters in the data due to difficulties in the acquisition and analysis of such measurements. The sun glitter data in clean water conditions compare well with the mean-square slope integrated from k_p to 316 rad/m, which does not extend into the capillary regime of the wave spectrum. In later theoretical analyses of the relationship between the surface wave spectrum and the mean-square slope [e.g., 10-11], it has been speculated that capillary waves may not contribute a significant portion to the ocean surface mean-square slope but a definitive proof remains unavailable. On the other hand, Ref. [12] evaluated the assumptions used in the data processing of sun glitter by Ref. [8] and concluded that the contribution from very steep surface slopes cannot be recovered from the mean-square slope data derived from the sun glitter measurements as processed. Thus the result reported in Ref. [8] only serves to provide a lower bound of the ocean surface mean-square slope. The analysis of intermediate-scale waves presented here seems to support that view point.

Ref. [9] derived the mean-square slope of the ocean surface from measurements of the airborne K_u-band altimeter backscattering data. Using their estimation of the diffraction limit of 0.1 m, the mean-square slope integrated from k_p to the corresponding wavenumber (62.8 rad/s) yields reasonable agreement with their analysis (Fig. 2).

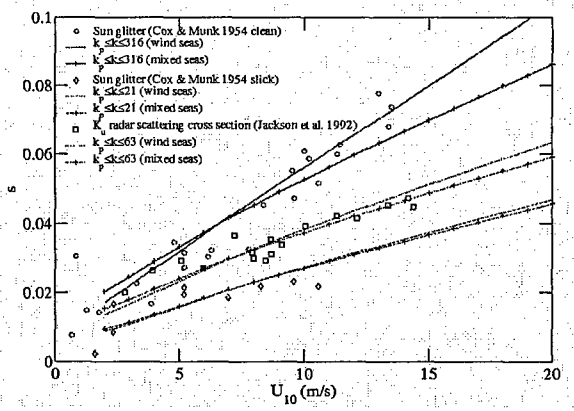

Fig. 2. Mean-square slopes integrated from k_p to different upper-bound wavenumbers, k_s. Field data from sun glitter and altimeter scattering analyses are also presented for comparison.

The wavenumber spectrum described here can be used to calculate the mean-square slopes of arbitrary wavenumber bands of surface gravity waves. The quantification of the band-pass filtered mean-square slopes, such as the tilting and Bragg scattering components of the sea surface roughness, are frequently needed in many remote sensing applications such as the computation of the radar scattering cross section and the modulation transfer function [e.g., 13-14].

IV. SUMMARY

Field measurements of intermediate-scale waves were obtained using a free-drifting measurement technique to reduce the complication in frequency-to-wavenumber conversion associated with Doppler frequency shift. Following an analysis by *Phillips* [1984] on the source function balance of surface waves, the dependence of the dimensionless spectrum, $B(k)$, on the dimensionless wind friction velocity, u_*/c, is investigated. The result shows that $B(u_*/c)$ can be represented by a power-law function. The proportionality coefficient, A_0, and the exponent, a_0, of the power-law function are determined from field data. The parameterization functions $A_0(k)$ and $a_0(k)$ can then be used to construct the wavenumber spectra of intermediate-scale waves at different wind speeds (Section 2). Using this spectral model, the band-pass filtered mean-square slope is derived. The calculated mean-square slopes are in good agreement with those obtained from analyses of sun glitter and K_u-band altimeter scattering cross sections. Empirically, it is found that the mean-square slope integrated from k_p to k_s ($k_s \geq \sim 10$ rad/m) increases approximately linearly with wind speed. The spectral model described here can be used for convenient computation of the band-pass filtered ocean surface roughness components frequently

needed in remote sensing applications.

ACKNOWLEDGEMENTS

This work is sponsored by the Office of Naval Research (NRL PE61153N). [NRL Contribution PP-7330--05-5202.]

REFERENCES

[1] Hwang, P. A., S. Atakturk, M. Sletten, and D. B. Trizna, A study of the wavenumber spectra of short water waves in the ocean, *J. Phys. Oceanogr.*, **26**, 1266-1285, 1996.

[2] Hara, T., Bock, E.J., Edson, J.B., McGillis, W.R., Observation of short wind waves in coastal waters, *J. Phys, Oceanogr.*, **28**, 1425-1438, 1998.

[3] Hwang, P. A., and D. W. Wang, An empirical investigation of source term balance of small scale surface waves, *Geophys. Res. Lett.*, **31**, L15301, doi:10.1029/2004GL20080, 2004.

[4] Phillips, O. M., On the response of short ocean wave components at a fixed wavenumber to ocean current variations, *J. Phys. Oceanogr.*, **14**, 1425-1433, 1984.

[5] Hwang, P. A., D. B. Trizna, and J. Wu, Spatial measurements of short wind waves using a scanning slope sensor, *Dyna. Atmos. and Oceans*, **20**, 1-23, 1993.

[6] Makin, V. K., and V. N. Kudryavtsev, Coupled sea surface-atmosphere model. 1. Wind over waves coupling, *J. Geophys. Res.*, **104**, 7613-7623, 1999.

[7] Makin, V. K., and V. N. Kudryavtsev, Impact of dominant waves on sea drag, *Bound.-Layer Meteorol.*, **103**, 83-99, 2002.

[8] Cox, C. S., and W. Munk, Statistics of the sea surface derived from sun glitter, *J. Mar. Res.*, **13**, 198-227, 1954.

[9] Jackson, F. C., W. T. Walton, D. E. Hines, B. A. Walter, and C. Y. Peng, Sea surface mean-square slope from K_u-band backscatter data, *J. Geophys. Res.*, **97**, 11411-11427, 1992.

[10] Plant, W. J., A relationship between wind stress and wave slope, *J. Geophys. Res.*, **87**, 1961-1967, 1982.

[11] Phillips, O. M., Spectral and statistical properties of the equilibrium range in wind-generated gravity waves, *J. Fluid Mech.*, **156**, 505-531, 1985.

[12] Wentz, F. J., Cox and Munk's sea surface slope variance, *J. Geophys. Res.*, **81**, 1607-1608, 1976.

[13] Plant, W. J., A two-scale model of short wind-generated waves and scatterometry, *J. Geophys. Res.*, **91**, 10735-10749, 1986.

[14] Plant, W. J., A model for microwave Doppler sea return at high incident angles: Bragg scattering from bound, tilted waves, *J. Geophys. Res.*, **102**, 21131-21146, 1997.